Tervalent-Metal Porphyrin-Phthalocyanine Heteroleptic Sandwich-Type Complexes. Synthesis, Structure, and Spectroscopic Characterization of Their Neutral, Singly-Oxidized, and Singly-Reduced States

D. Chabach,[†,‡] M. Tahiri,[†,‡] A. De Cian,[†] J. Fischer,[†] R. Weiss,*[,†] and M. El Malouli Bibout[‡]

Contribution from the Laboratoire de Cristallochimie et de Chimie Structurale (URA 424), Institut Le Bel, Université Louis Pasteur, 67000 Strasbourg, France, and Faculté des Sciences Aïn Chock, Université Hassan II, B.P. 5366 Maarif, Casablanca, Morroco

Received December 14, 1994[⊗]

Abstract: The synthesis and spectroscopic properties of the neutral metal(III) heteroleptic porphyrin-phthalocyanine double-decker sandwich-like complexes |(TPP)M^{III}(Pc)| (**1**) are reported (TPP and Pc = dianions of tetraphenylporphyrin and phthalocyanine, respectively; M = La, Pr, Nd, Eu, Gd, Er, Lu, and Y). The electron transfer reactions of these M^{III} complexes are presented. They undergo up to four reversible one-electron transfers in nonaqueous media. The spectroscopic properties of these |(TPP)M^{III}(Pc)| (**1**) sandwich-like derivatives are consistent with the presence of a one-electron-oxidized π-radical phthalocyanine ring, $Pc^{\bullet-}$, as a ligand. Accordingly, these π-radical complexes **1** yield monoanionic species |(TPP)M^{III}(Pc)|$^-$ **2** upon reversible one-electron reduction and di-π-radical complexes |(TPP)M^{III}(Pc)|$^+$ **3** containing a tetraphenylporphyrin π-radical and a phthalocyanine π-radical ligand upon reversible one-electron oxidation. In the neutral complexes **1** and the di-π-radical derivatives **3**, the energies of the near-infrared bands are linearily correlated with the ionic radii r_i of the tervalent central metals. A decrease of the two reversible one-electron reduction and the first reversible oxidation potentials parallels a decrease of the ionic radii and, hence, the ring-ring separations in these sandwich double-decker species. A protonated lanthanum derivative, |(TPP)LaH(Pc)| (**1**[H](La)), has been isolated which shows an IR spectral band at 3280 cm^{-1}, consistent with an N-H stretching vibration corresponding to a protonated tetrapyrrole ligand. The crystal and molecular structures of the lanthanum derivative |(TPP)La(Pc)|·$2CH_2Cl_2$ (**1**(La)·$2CH_2Cl_2$) and the singly-oxidized gadolinium species |(TPP)Gd(Pc)||$SbCl_6$|·$2(CH_2Cl_2)$,(H_2O) (**3**(Gd)($SbCl_6$)·$2(CH_2Cl_2)$,(H_2O)) have been established. Crystal data: **1**(La)·$2CH_2Cl_2$, monoclinic, $P2_1/c$, a = 12.935(5) Å, b = 18.674(6) Å, c = 26.114(9) Å, β = 90.90(2)°, Z = 4; **3**(Gd)($SbCl_6$)·$2(CH_2Cl_2)$,(H_2O), triclinic, $P\bar{1}$, a = 18.190(5) Å, b = 16.100(5) Å, c = 14.130(4) Å, α = 104.87(2)°, β = 104.17(2)°, γ = 107.72(2)°, Z = 2. These studies confirm the double-decker sandwich-type structures of these derivatives.

Introduction

The neutral lanthanide(III) bis(phthalocyanine) and bis(porphyrin) complexes, displaying a double-decker sandwich-type structure, contain a one-electron-oxidized π-radical tetrapyrrole ring as a ligand.[1] Due to the strong π-π interactions of the two tetrapyrrole ligands in these homoleptic sandwich-type complexes, the unpaired spin is delocalized over the two identical tetrapyrrole rings.[2] Recently, several groups have reported the preparation and properties of several heteroleptic sandwich-type complexes: |(TPP)Ce^{IV}(Pc)|,[3] |(TPP)Ce^{IV}(OEP)|,[4] |(TTP)Ce^{IV}(OEP)|,[5] |(OEP)Zr^{IV}(salen)|,[6] |(P)U^{IV}(Pc)|, and |(P)-Th^{IV}(Pc)| (P = dianions of octaethylporphyrin (OEP), tetraphenylporphyrin (TPP), or tetra-*p*-tolylporphyrin (TTP)).[7] It has been shown that in |(TPP)Ce^{IV}(Pc)|$^+$ the electronic hole preferentially resides on the phthalocyanine ring[8] and in |(TPP)Ce^{IV}(OEP)|$^+$ and |(TPP)Eu^{III}(OEP)| on the octaethylporphyrin rings.[4,9] These results are consistent with the oxidation potentials known for monomeric metallophthalocyanine and metallooctaethylporphyrin derivatives relative to the oxidation potentials of the metallotetraphenylporphyrin complexes. In order to investigate the electronic properties of heteroleptic sandwich-type metalloporphyrin-phthalocyanine derivatives in which the metal keeps the oxidation state III, we have synthesized and studied the structural and spectroscopic properties of |(TPP)M(Pc)| (**1**) complexes with M = La, Pr, Nd, Eu, Gd, Er, Lu, and Y. Herein we report the results of these studies.

Experimental Section

Chemicals. All chemicals were of reagent grade and were used without further purification except as noted below. H_2TPP,[10,11] Li_2-Pc,[12] M(acac)$_3$·nH_2O (M = La, Pr, Nd, Eu, Gd, Er, Lu, and Y),[13] and

[†] Université Louis Pasteur.
[‡] Université Hassan II.
[⊗] Abstract published in *Advance ACS Abstracts*, July 15, 1995.

(1) (a) Kirin, I. S.; Moskalev, Yu. A. *Russ. J. Inorg. Chem. (Engl. Transl.)* **1965**, *10*, 1065. (b) Chang, A. T.; Marchon, J. C. *Inorg. Chim. Acta* **1981**, *53*, L-241. (c) Buchler, J. W.; De Cian, A.; Fischer, J.; Kihn-Botulinski, M.; Paulus, H.; Weiss, R. *J. Am. Chem. Soc.* **1986**, *108*, 3652. (d) Buchler, J. W.; Scharbert, B. *J. Am. Chem. Soc.* **1988**, *110*, 4272.

(2) (a) De Cian, A.; Moussavi; M.; Fischer, J.; Weiss, R. *Inorg. Chem.* **1985**, *24*, 3162. (b) Buchler, J. W.; De Cian, A.; Fischer, J.; Kihn-Botulinski, M.; Weiss, R. *Inorg. Chem.* **1988**, *27*, 339.

(3) Lachkar, M.; De Cian, A.; Fischer, J.; Weiss, R. *New J. Chem.* **1988**, *12*, 729.

(4) Buchler, J. W.; De Cian, A.; Fischer, J.; Hammerschmitt, P.; Löffler, J.; Scharbert, B.; Weiss, R. *Chem. Ber.* **1989**, *122*, 2219.

(5) Bilsel, O.; Rodriguez, J.; Holten, D. *J. Phys. Chem.* **1990**, *94*, 3508.

(6) Buchler, J. W.; Hammerschmitt, P. *Liebigs Ann. Chem.* **1991**, 1177.

(7) Kadish, K. M.; Moninot, G.; Hu, Y.; Dubois, D.; Ibnlfassi, A.; Barbe, J. M.; Guillard, R. *J. Am. Chem. Soc.* **1993**, *115*, 8153.

(8) Tran-Thi, T. H.; Mattioli, T.; Chabach, D.; De Cian, A.; Weiss, R. *J. Phys. Chem.* **1994**, *98*, 8279.

(9) Buchler, J. W.; Löffler, J. *Z. Naturforsch.* **1990**, *45b*, 531.

(10) Adler, A. D.; Longo, F. R.; Finarelli, J. D.; Goldmacher, J.; Assour, J.; Korsakoff, L. *J. Org. Chem.* **1967**, *32*, 476.

(11) Barnett, G. H.; Hudson, M. F.; Smith, K. M. *J. Chem. Soc., Perkin Trans. 1* **1975**, 1401.

0002-7863/95/1517-8548$09.00/0

phenoxathiinylium hexachloroantimonate[14] were synthesized and purified according to literature methods. Dichloromethane (CH_2Cl_2) and hexane were distilled from CaH_2 under an atmosphere of nitrogen. CH_2Cl_2 was freed from traces of acids with basic alumina. 1,2,4-Trichlorobenzene (TCB; Fluka) was purified with basic alumina. Chromatographic separations were performed on silica gel columns (0.040–0.063 mm, Merck). The purity of the products was checked by thin layer chromatography. The supporting electrolyte tetrabutylammonium hexafluorophosphate (NBu_4PF_6) (Fluka) was recrystallized twice from ethanol and dried at 100 °C under vacuum.

Methods and Instruments. All manipulations of oxygen and water sensitive materials were performed with Schlenkware and cannula techniques under an argon atmosphere. Ultraviolet–visible (UV–vis) and near-infrared (near-IR) spectra were recorded on a CARY 219 spectrophotometer. Infrared spectra were obtained on an IFS 66 Bruker spectrophotometer (KBr pellets, 4000–400 cm^{-1}). The EPR spectrometer was a conventional X-band apparatus (Bruker ER 200 D). The g value was measured relative to diphenylpicrylhydrazyl (DPPH) ($g = 2.0037 \pm 0.0002$). Elemental analyses were performed by the Service de Microanalyse de l'Université Louis Pasteur de Strasbourg. All electrochemical measurements were carried out with a conventional three-electrode system. A platinum-button electrode was used as the working electrode, a platinum wire as the counter electrode. The reference electrode was a homemade saturated calomel electrode (SCE) which was separated from the working solution by a fritted glass bridge. Cyclic voltammetry experiments were carried out with Princeton Applied Research equipment (PAR 273A and PAR software). To eliminate traces of water, the solvent was treated with Al_2O_3 in the electrochemical cell. All solutions were deoxygenated by passing a stream of argon for at least 15 min prior to recording the voltammogram. To maintain an O_2-free environment, the solution was blanketed with argon during all experiments. Cyclic voltammograms were obtained with 5×10^{-4} M solutions of the samples in 0.1 M NBu_4PF_6 in CH_2Cl_2. All the potentials reported herein were measured at 25 °C and are given relative to the potential of the saturated calomel electrode (SCE).

Synthetic Procedures. Depending on the radius of the metal cation, the preparation of the heteroleptic double-decker sandwich-type complexes |(TPP)M(Pc)| (**1**) (M = La, Pr, Nd, Eu, Gd, Er, Lu, and Y) was achieved using two slightly different methods. With the larger metal cations (La–Gd) the heteroleptic sandwiches were obtained by substitution of the acetylacetonate ligand by tetraphenylporphyrin in the monophthalocyanine |(Pc)M(acac)| derivatives.[15] With the smaller metal cations (Er, Lu, and Y), the nonsymmetrical sandwiches were prepared by substitution of the acetylacetonate ligand by phthalocyanine in the monoporphyrin species |(TPP)Ln(acac)|.[16,17]

Synthesis of |(TPP)M(Pc)| Complexes with M = La, Pr, Nd, Eu, and Gd. A 790 mg (1.5 mmol) sample of dilithium phthalocyanine (Li_2Pc) and 2.5 mmol of metal acetylacetonate ($M(acac)_3 \cdot nH_2O$ (M = La, Pr, Nd, Eu, Gd)) were added to 1,2,4-trichlorobenzene (TCB) (80 mL) in a three-neck flask equipped with a reflux condenser, and the mixture was heated to 120 °C over a 3 h period under a slow stream of argon. To this solution was added, after cooling under argon, 920 mg (1.5 mmol) of tetraphenylporphyrin (H_2TPP), and the whole mixture was heated to reflux. The reaction progress was monitored by UV–vis spectroscopy and TLC, and refluxing was stopped after 8 h. The mixture was allowed to cool slowly to room temperature, and the flask was opened to the atmosphere. The TCB was removed in vacuo, and the residue was extracted with dichloromethane (several times). The extracts were combined and concentrated under vacum to give a solution which was purified by column chromatography (silica gel, 4–30 cm). For all the metals (except lanthanum), elution with toluene yielded successively the red-brown metal(III) tetraphenylporphyrin–phthalocyanine double-decker derivatives |(TPP)M(Pc)| (**1**) (major fraction) and an olive-green bismetal(III) bis(tetraphenylporphyrin–phthalocyanine) triple-decker complex, |(TPP)M(Pc)M(TPP)| (minor fraction).[18] The major fraction was concentrated under vacuum, and the red-brown mixed-ligand derivatives **1** (M = La, Pr, Nd, Eu, Gd) were precipitated by addition of hexane.

All compounds were stable in air and gave analytical and spectral results in agreement with a 1:1:1 metal/porphyrin/phthalocyanine formulation.

|(TPP)Pr(Pc)|: 810 mg (42.7%). Anal. Calcd for $C_{76}H_{44}N_{12}Pr$: C, 72.09; H, 3.50; N, 13.27. Found: C, 71.87; H, 3.53; N, 12.98.

|(TPP)Nd(Pc)|: 894 mg (47%). Anal. Calcd for $C_{76}H_{44}N_{12}Nd$: C, 71.90; H, 3.49; N, 13.24. Found: C, 71.32; H, 3.51; N, 13.07.

|(TPP)Eu(Pc)|: 1110 mg (58%). Anal. Calcd for $C_{76}H_{44}N_{12}Eu$: C, 71.4; H, 3.47; N, 13.16. Found: C, 71.29; H, 3.44; N, 13.05.

|(TPP)Gd(Pc)|: 1076 mg (56%). Anal. Calcd for $C_{76}H_{44}N_{12}Gd$: C, 71.18; H, 3.46; N, 13.12. Found: C, 70.86; H, 3.51; N, 13.04.

When the metal cation is lanthanum(III), a light-green protonated species, |(TPP)LaH(Pc)|, was obtained (see Discussion). Unreacted H_2TPP and the olive-green triple-decker derivative |(TPP)La(Pc)La(TPP)| were first eluted with toluene, and then a light-green fraction was eluted with dichloromethane. The eluate was precipitated, the solvent removed, and the solid dried in vacuo.

|(TPP)LaH(Pc)|: 682 mg (36%). Anal. Calcd for $C_{76}H_{45}N_{12}La$: C, 72.15; H, 3.58; N, 13.29. Found: C, 70.89; H, 3.64; N, 13.21. IR: 3280 cm^{-1}. Near-IR: no absorption. MS: m/z = 1265.2 (calcd 1265.17 for ^{139}La).

Synthesis of |(TPP)M(Pc)| Complexes with M = Er, Lu, and Y. The reaction was carried out by using a three-neck flask equipped with a reflux condenser. A mixture containing 300 mg (0.49 mmol) of H_2TPP and 400 mg (0.8 mmol) of $M(acac)_3 \cdot nH_2O$ (M = Er, Lu, Y) in 80 mL of TCB was stirred and heated to reflux under argon. The progress of the reaction was monitored by UV–vis spectroscopy and TLC. After 4 h, the reaction mixture was allowed to cool under a slow stream of argon. A 316 mg (0.6 mmol) sample of Li_2Pc was added, and the mixture was refluxed for 8 h. Cooling of the solution and addition of hexane yielded a crude solid. Chromatography on a silica gel column (4–30 cm) with toluene as the solvent yielded two fractions. The first one, in minor quantity, corresponded to unreacted H_2TPP. The second fraction (major) contained the red-brown double-decker derivatives **1** (M = Er, Lu, and Y), which were precipitated by addition of hexane.

|(TPP)Er(Pc)|: 530 mg (83.6%). Anal. Calcd for $C_{76}H_{44}N_{12}Er$: C, 70.62; H, 3.43; N, 13.00. Found: C, 70.56; H, 3.46; N, 12.87.

|(TPP)Lu(Pc)|: 547 mg (86%). Anal. Calcd for $C_{76}H_{44}N_{12}Lu$: C, 70.21; H, 3.41; N, 12.93. Found: C, 69.93; H, 3.36; N, 12.34.

|(TPP)Y(Pc)|: 505 mg (85%). Anal. Calcd for $C_{76}H_{44}N_{12}Y$: C, 75.18; H, 3.65; N, 13.84. Found: C, 74.96; H, 3.62; N, 13.71.

Oxidation of the Protonated Form |(TPP)LaH(Pc)| (1[H](La)) to |(TPP)La(Pc)| (1(La)): A saturated solution of phenoxathiinylium hexachloroantimonate in dichloromethane was added portionwise with a cannula to a solution of |(TPP)LaH(Pc)| in pyridine/dichloromethane (1:1). The progress of the reaction was followed by UV–vis/near-IR spectroscopy and TLC and the addition of oxidizing reagent terminated when the constant spectrum of |(TPP)La(Pc)| was observed. During the reaction, a color change from light-green to red-brown was observed. The solvent was removed under vacuum. Recrystallization from CH_2Cl_2/hexane yielded |(TPP)La(Pc)| (57%). The nature of this complex was confirmed by spectroscopy and by an X-ray structure determination (vide infra).

One-Electron Chemical Reduction of |(TPP)M(Pc)| (1). A 20 mg sample of **1** was dissolved in 30 mL of CH_2Cl_2/NBu_4PF_6. An excess of $N_2H_4 \cdot H_2O$ was added and the mixture stirred for 30 min. Addition of hexane yielded the one-electron-reduced states $|(TPP)M(Pc)|^-|NBu_4|^+$ (**2**).

One-Electron Electrochemical Reduction of |(TPP)M(Pc)| (1). A solution of about 5 mmol of **1** in 50 mL of CH_2Cl_2 containing NBu_4PF_6 (0.1 M) was electrolyzed at a constant potential of −0.1 V (vs SCE) to give the one-electron-reduced species $|(TPP)M(Pc)|^-|NBu_4|^+$

(12) Barrett, R. A.; Frye, D. A.; Linstead, R. P. *J. Chem. Soc.* **1938**, 1157.
(13) Stites, J. G.; Mc Carty, C. N.; Quill, L. L. *J. Am. Chem. Soc.* **1948**, *70*, 3142.
(14) Gans, P.; Marchon, J. C.; Reed, C. A.; Regnard, J. R. *Nouv. J. Chim.* **1981**, *5*, 203.
(15) Sugimoto, H.; Higashi, T.; Mori, M. *Chem. Lett.* **1982**, 801.
(16) Wong, C. P.; Venteicher, R. F.; Horrocks, W. DeW., Jr. *J. Am. Chem. Soc.* **1974**, *96*, 7149.
(17) Buchler, J. W.; Eickelmann, G.; Puppe, L.; Rohbock, K.; Schneehage, H. H.; Weck, D. *Liebigs Ann. Chem.* **1971**, *745*, 135.
(18) Chabach, D.; Lachkar, M.; De Cian, A.; Fischer, J.; Weiss, R. *New J. Chem.* **1992**, *16*, 431.

Table 1. Summary of Single Crystal X-ray Diffraction Data

	1(La)·2CH_2Cl_2	**3**(Gd)($SbCl_6$)·2(CH_2Cl_2),(H_2O)
formula	$C_{78}H_{48}Cl_4N_{12}La$	$C_{78}H_{50}Cl_{10}N_{12}OSbGd$
mol wt	1434	1805
color	violet	dark green
crystal system	monoclinic	triclinic
a (Å)	12.938(5)	18.190(5)
b (Å)	18.674(6)	16.100(5)
c (Å)	26.114(9)	14.130(4)
α (deg)	90	104.87(2)
β (deg)	90.90(2)	104.17(2)
γ (deg)	90	107.72(2)
V (Å^3)	6308.5	3567.7
Z	4	2
d_{calcd} (g cm^{-3})	1.509	1.680
λ (Å)	1.5418	1.5418
μ (cm^{-1})	73.439	133.676
space group	$P2_1/c$	$P\bar{1}$
diffractometer	Philips PW1100/16	Philips PW1100/16
crystal dimens (mm)	0.34 × 0.20 × 0.20	0.25 × 0.15 × 0.15
temperature (°C)	−100	−100
radiation	Cu Kα (graphite monochromated)	Cu Kα (graphite monochromated)
mode	$\theta/2\theta$ (flying step scan)	$\theta/2\theta$ (flying step scan)
scan speed (deg)	0.020	0.020
step width (deg)	0.04	0.03
scan width (deg)	0.90 + 0.14 tan(θ)	0.80 + 0.14 tan(θ)
octants	$\pm h, +k, +l$	$\pm h, \pm k, +l$
θ min/max (deg)	3/52	3/52
no. of data collected	7543	7522
no. of data with $I \geq 3\sigma(I)$	6153	6325
abs min/max	0.92/1.09	0.89/1.22
$R(F)$	0.025	0.047
$Rw(F)$	0.044	0.075
P	0.08	0.08
GOF	1.039	1.708

(**2**). The reaction was accompanied by a color change from red-brown to light-green. Samples were withdrawn and diluted for measurement of their UV−vis spectra. Besides bands of |(TPP)M(Pc)|$^-$|NBu_4|$^+$, no bands of H_2TPP appeared, indicating no demetalation of the double-decker derivatives.

One-Electron Chemical Oxidation of |(TPP)M(Pc)| (1). A solution of **1** (15 mmol) in CH_2Cl_2 (ca. 30 mL) was treated with 1.1 equiv of phenoxathiinylium hexachloroantimonate. The reaction was accompanied by a color change from red-brown to red and monitored by UV−vis and near-IR spectroscopy. After completion of the reaction, the solvent was removed in vacuo. Recrystallization from CH_2Cl_2/hexane yielded the one-electron-oxidized species |(TPP)M(Pc)|$^+$|$SbCl_6$|$^-$ (**3**) (yield 60−70%).

One-Electron Electrochemical Oxidation of |(TPP)M(Pc)| (1). A solution of about 5 mmol of **1** in 50 mL of CH_2Cl_2/NBu_4PF_6 was electrolyzed at +0.70 V with simultaneous sonification of the electrolysis cell. Within 40 min, the current dropped to 0.003 mV. Formation of the singly-oxidized species |(TPP)M(Pc)|$^+$ **3** was checked by UV−vis and near-IR spectroscopy.

X-ray Analyses of 1(La)·2CH_2Cl_2 and 3(Gd)($SbCl_6$)·2(CH_2Cl_2),(H_2O). Single crystals suitable for X-ray studies were obtained by slow diffusion of hexane into dichloromethane solutions of the compounds. Crystal data, data collection parameters, and refinement results for **1**(La)·2CH_2Cl_2 and **3**(Gd)($SbCl_6$)·2(CH_2Cl_2),(H_2O) are displayed in Table 1. Data were collected at −100 °C on a Philips PW 1100/16 automatic diffractometer equipped with a locally built low-temperature device. The resulting data sets were transferred to a VAX computer, and for all subsequent calculations the Enraf-Nonius Molen/VAX package[19] was used with the exception of a local data reduction program. Three standard reflections measured every hour during the entire data collection periods showed no significant trend. The raw step-scan data were converted to intensities using the Lehmann−Larsen method,[20] and corrected for Lorentz and polarization factors. The structures were solved by the heavy-atom method. After refinement of the atoms, a difference Fourier map revealed maxima of residual electron density close to the positions accepted for the hydrogen atoms; they were introduced in structure factor calculations by their computed coordinates for carbon-bonded hydrogen (C−H = 0.95 Å) and isotopic temperature factors such as B(H) = 1.3 + B(eqv)(C) Å^2. No hydrogen atom parameter was allowed to vary during full-matrix least-squares refinements minimizing $\sum w(|F_o| - |F_c|)^2$. Before anisotropic refinements of the non-hydrogen atoms, empirical absorption corrections were applied using the method of Walker and Stuart.[21] No extinction corrections were applied. The unit weight observations are for p = 0.08 in $w = 1/(\sigma$ counts + $(pI)^2)$. The final difference map revealed no significant maxima. The scattering factor coefficients and anomalous dispersion coefficients come, respectively, from refs 22a and 22b.

Results and Discussion

The work of J. Buchler et al.[4,9,23,24] indicated that the lanthanide bisporphyrins |(TPP)Ln(TPP)| are easier to isolate and more stable with the larger lanthanides (Ln = lanthanide). By contrast, the lanthanide bisphthalocyanines |(Pc)Ln(Pc)| are easier to obtain and more stable with the smaller lanthanide cations.[1a,25] Accordingly, as already indicated in the Experimental Section, in order to isolate the neutral forms of the heteroleptic metal(III) porphyrin−phthalocyanine |(TPP)M(Pc)| derivatives (**1**), we have adopted two different strategies: With the larger metal cations (La−Gd), we reacted the metal-free

(19) Molen. *An Interactive Structure Solution Procedure*; Enraf-Nonius: Delft, The Netherlands, 1990.

(20) Lehmann, M. S.; Larsen, F. K. *Acta Crystallogr., Sect. A: Cryst. Phys., Diffr., Theor. Gen. Crystallogr.* **1974**, *A30*, 580.

(21) Walker, N.; Stuart, D. *Acta Crystallogr., Sect. A: Fundam. Crystallogr.* **1983**, *A39*, 159.

(22) Cromer, D. T.; Waber, J. T. *International Tables for X-ray Crystallography*; Kgnoch: Birmingham, England, 1974; Vol. IV, (a) Table 2.2.b, (b) Table 2.3.1.

(23) Buchler, J. W.; Kapellmann, H. G.; Knoff, M.; Lay, K. L.; Pfeifer, S., *Z. Naturforsch.* **1983**, *38B*, 1339.

(24) Buchler, J. W.; Hammerschmitt, P.; Kaufeld, I.; Löffler, J. *Chem. Ber.* **1991**, *124*, 2151.

(25) Clarisse, C.; Riou, M. T. *Inorg. Chim. Acta* **1987**, *130*, 139.

Table 2. (a) UV–Vis and Near-IR Band Maxima of |(TPP)M(Pc)| (**1**), (b) UV–Vis Band Maxima of |(TPP)M(Pc)|$^-$ **2**, and (c) UV–Vis and Near-IR Band Maxima of |(TPP)M(Pc)|$^+$ **3**

(a) |(TPP)M(Pc)| (**1**)

	λ(nm) (log ε)				
M = La	324 (4.65)	412 (5.37)	484 (4.15)	965 (3.24)	1535 (3.38)
Pr	325 (4.72)	410 (5.28)	480 (3.98)	968 (3.27)	1469 (3.36)
Nd	326 (4.66)	410 (5.39)	476 (4.07)	995 (3.31)	1434 (3.43)
Eu	326 (4.69)	408 (5.26)	476 (4.13)	1002 (3.25)	1350 (3.41)
Gd	327 (4.71)	406 (5.31)	472 (3.87)	1005 (3.21)	1321 (3.39)
Y	328 (4.65)	402 (5.18)	472 (4.21)	1053 (3.23)	1285 (3.37)
Er	328 (4.71)	400 (5.20)	470 (3.88)	1057 (3.19)	1255 (3.35)
Lu	328 (4.68)	396 (5.13)	468 (3.97)	1067 (3.22)	1211 (3.38)

(b) |(TPP)M(Pc)||NBu_4| (**2**)

	λ (nm) (log ε)							
M = La	336 (4.92)	380 (4.51)	418 (5.78)	482 (4.23)	576 (3.81)	602 (3.85)	630 (3.58)	746 (3.66)
Pr	336 (4.97)	379 (4.58)	416 (5.81)	479 (4.31)	574 (3.80)	598 (3.89)	636 (3.71)	770 (3.64)
Nd	337 (5.01)	382 (4.54)	414 (5.79)	483 (4.27)	577 (3.75)	604 (3.83)	644 (3.65)	784 (3.68)
Eu	337 (4.84)	381 (4.49)	413 (5.68)	481 (4.21)	578 (3.77)	601 (3.81)	644 (3.68)	785 (3.74)
Gd	335 (4.89)	388 (4.52)	410 (5.70)	478 (4.23)	577 (3.74)	603 (3.79)	638 (3.65)	788 (3.64)
Y	338 (4.86)	384 (4.48)	410 (5.66)	480 (4.20)	575 (3.73)	600 (3.80)	648 (3.59)	843 (3.64)
Er	336 (4.85)	382 (4.48)	409 (5.62)	479 (4.18)	574 (3.71)	602 (3.83)	649 (3.62)	843 (3.70)
Lu	337 (4.80)	381 (4.41)	410 (5.60)	480 (4.21)	577 (3.69)	606 (3.78)	647 (3.69)	850 (3.65)

(c) |(TPP)M(Pc)||$SbCl_6$| (**3**)

	λ (nm) (log ε)			
M = La	326 (5.20)	406 (5.13)	472 (4.39)	1183 (3.77)
Pr	328 (5.12)	406 (5.08)	470 (4.45)	1140 (3.81)
Nd	326 (5.18)	403 (5.10)	468 (4.42)	1140 (3.83)
Eu	328 (5.14)	402 (5.13)	470 (4.36)	1080 (3.73)
Gd	329 (5.08)	403 (4.98)	467 (4.31)	1072 (3.70)
Y	332 (5.11)	400 (4.91)	468 (4.38)	1031 (3.65)
Er	332 (5.03)	400 (4.94)	468 (4.36)	1027 (3.68)
Lu	330 (5.12)	397 (4.93)	466 (4.37)	1006 (3.64)

Scheme 1. Synthesis of Heteroleptic Sandwich Complexes |(TPP)M(Pc)| (**1**) (M = La, Pr, Nd, Eu, Gd)

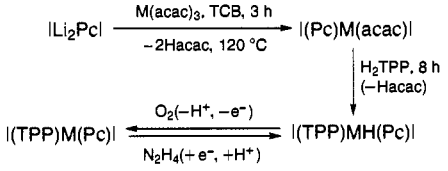

Scheme 2. Synthesis of Heteroleptic Sandwich Complexes |(TPP)M(Pc)| (**1**) (M = Er, Lu, Y)

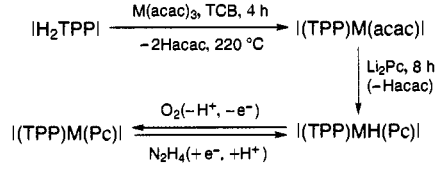

tetraphenylporphyrin (H_2TPP) with the monophthalocyanine derivative |(Pc)M(acac)| (Scheme 1).

With the smaller metal cations (M = Er, Lu, and Y), we reacted the dilithium phthalocyanine (Li_2Pc) with the monoporphyrin complex |(TPP)Ln(acac)| (Scheme 2).

Most probably, the protonated forms |(TPP)MH(Pc)| (**1**[H]) are a common intermediate. However, such an intermediate could only be isolated with M = La. With the other metal cations, the neutral form |(TPP)M(Pc)| (**1**) contains a tetrapyrrole π-radical monoanion as a ligand which results, most probably, by oxidation of the protonated forms **1**[H] by O_2 (Schemes 1 and 2). The yields of formation of the neutral form **1** of the heteroleptic sandwiches increase when the metal cation radii decrease. The preparation becomes almost quantitative, with the metal cation displaying the smallest radius (Lu) (see Experimental Section).

Spectroscopic Properties of the |(TPP)M(Pc)| Complexes (1) (M = La, Pr, Nd, Eu, Gd, Er, Lu, and Y). The maxima (λ nm, log ε) of the bands appearing in the UV–vis absorption spectra of the heteroleptic |(TPP)M(Pc)| derivatives (**1**), in dichloromethane, are displayed in Table 2a. Figure 1a shows the absorption spectrum of |(TPP)Eu(Pc)|, which is representative for the spectra of these compounds. By analogy with the homoleptic bisphthalocyanine |(Pc)M(Pc)| and bis(tetraphenylporphyrin) |(TPP)M(TPP)| tervalent-metal sandwich derivatives,[1b,24,25,26] the band lying between 324 and 328 nm in the spectra of the |(TPP)M(Pc)| derivatives is attributed to the phthalocyanine Soret band and the band appearing between 396 and 412 nm to the porphyrin Soret band. The phthalocyanine Q bands lying between 500 and 700 nm in the spectra of the bisphthalocyanine tervalent-metal derivatives |(Pc)M(Pc)| are absent in the absorption spectra of the heteroleptic |(TPP)M(Pc)| derivatives. In contrast, two bands lying, respectively, between 468 and 484 nm and 965 and 1067 nm appear in these spectra (see Table 2a). These bands have counterparts in the spectra of the homoleptic |(Pc)M(Pc)| tervalent-metal derivatives. Their presence in these spectra has been ascribed to an electron hole in the a_{1u} orbital of one phthalocyanine ring and to correspond to $2e_g \rightarrow a_{1u}$ and $1e_g \rightarrow a_{1u}$ transitions, respectively.[27] Consequently, the corresponding bands in the heteroleptic |(TPP)M(Pc)| sandwich derivatives can also be attributed to an electron hole localized on the phthalocyanine

(26) (a) Collins, G. C. S.; Schiffrin, D. *J. Electroanal. Chem.* **1982**, *139*, 335. (b) l'Her, M.; Cozien, Y.; Courtot-Coupez, J. *Compt. Rend. Acad. Sci. (Paris)* **1985**, *300*, 487.

(27) Markovitsi, D.; Tran-Thi, T. H.; Even, R.; Simon, J. *Chem. Phys. Lett.* **1987**, *137*, 107.

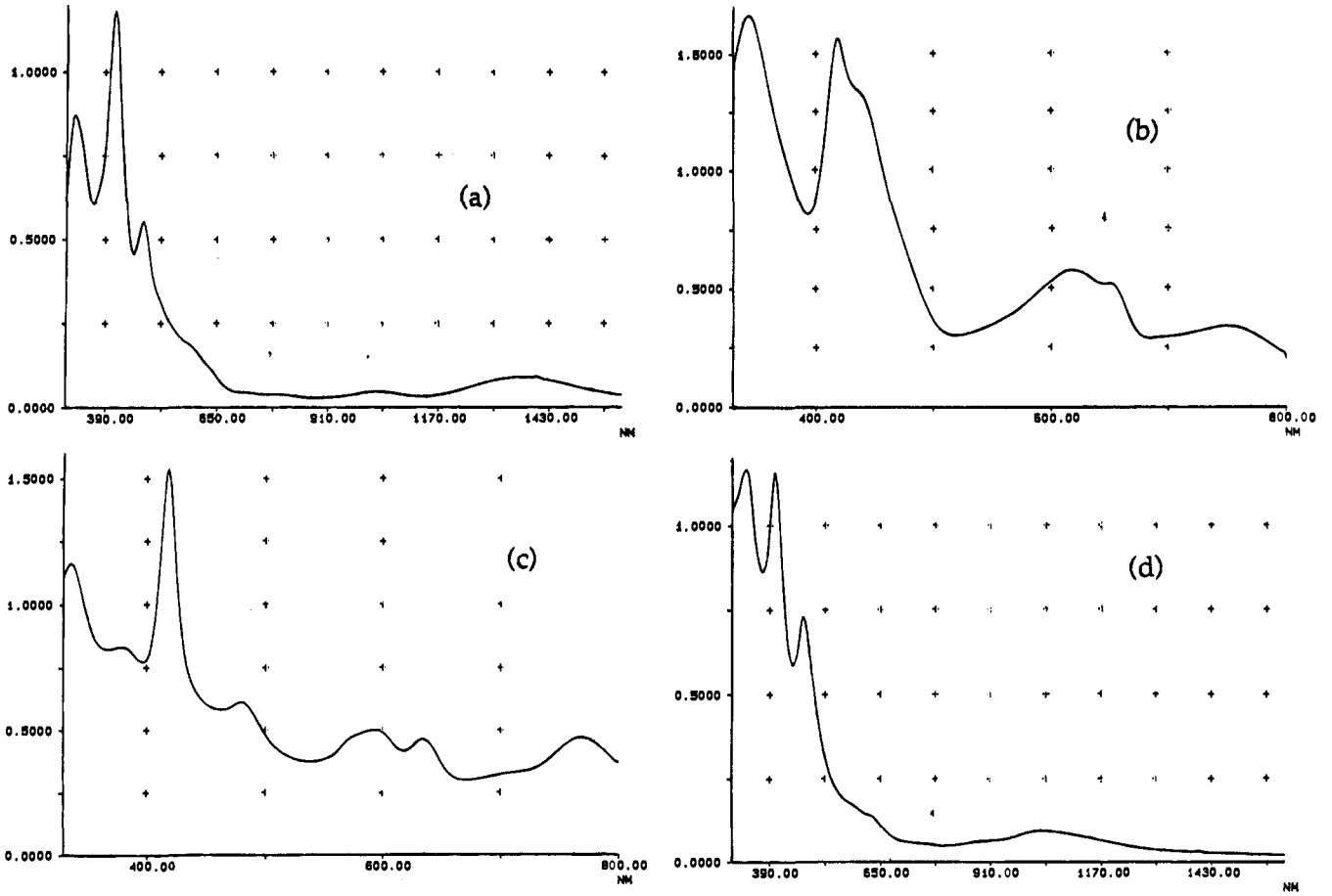

Figure 1. UV−vis spectra in dichloromethane of (a) |(TPP)Eu(Pc)| (**1**(Eu)) and (b) |(TPP)LaH(Pc)| (**1**(H)(La)), |(TPP)Pr(Pc)|$^-$ **2**(Pr), and |(TPP)-Er(Pc)|$^+$ **3**(Er).

ring with identical assignments. Furthermore, a broad band appears in the near-IR in the spectra of the heteroleptic sandwich derivatives |(TPP)M(Pc)|. The maxima of these near-IR bands lie between 1211 (Lu) and 1535 (La) nm, depending on the nature of the tervalent-metal cation. Such a band has also been observed in the homoleptic |(Pc)M(Pc)|[27] and |(Po)M(Po)| (Po = tetraphenylporphyrin, TPP, and octaethylporphyrin, OEP) and heteroleptic |(TPP)Ce^{IV}(OEP)|$^+$ derivatives.[1d,4,24] As in these bisphthalocyanine and bisporphyrin complexes, when the ionic radius of the tervalent-metal cation increases, the absorption maximum of the near-IR band of |(TPP)M(Pc)| is shifted to longer wavelengths: a linear correlation (Figure 2a) is observed between the wavenumbers of these bands and the M^{III} ionic radii r_i,[28] indicating that the energies of the near-IR transitions depend on the ring to ring separations occurring between the two tetrapyrrole macrocycles. This band which lies at 1382 nm in the absorption spectrum of |(Pc)Lu(Pc)| has been attributed to an intramolecular charge transfer transition in which the Pc^{2-} anionic ligand acts as an electron donor and the radical monoanionic Pc$^{\bullet-}$ ligand as an electron acceptor. By analogy with this near-IR band appearing in the absorption spectrum of |(Pc)Lu(Pc)|, the near-IR band appearing between 1211 and 1535 nm in the spectra of the heteroleptic |(TPP)M(Pc)| species can be ascribed to an intramolecular charge transfer transition in which the TPP^{2-} dianionic ligand acts as an electron donor and the monoanionic Pc$^{\bullet-}$ radical as the electron acceptor.

However, the presence of such a near-IR band and the linear correlation of the wavenumbers of these bands with the ionic radii of the metal cations suggest also that $\pi-\pi$ interactions

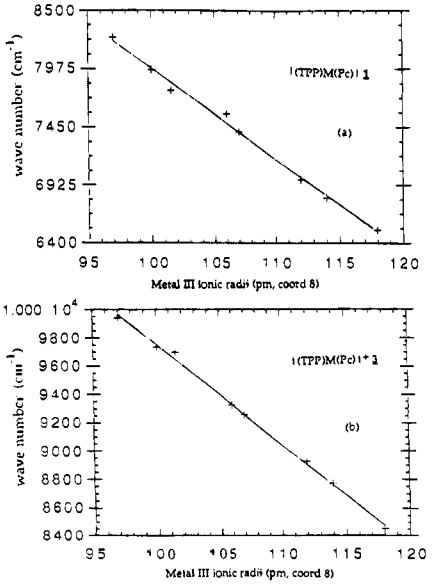

Figure 2. Wavenumbers of the near-IR absorption maxima of the heteroleptic sandwich complexes as a function of the ionic radii r_i (pm; octacoordinated) of tervalent central metal M: (a) |(TPP)M(Pc)| (**1**) and (b) |(TPP)M(Pc)|$^+$ **3**.

are still present between the two different tetrapyrrole ligands of these complexes. Such $\pi-\pi$ interactions are present in the homoleptic metal bisphthalocyanine and bisporphyrin sandwich derivatives,[24,29] and are probably also present in the heteroleptic |(OEP)Ce^{IV}(TPP)| and |(OEP)Ce^{IV}(TPP)|$^+$ derivatives.[30] Since their molecular structures are similar, the molecular orbital diagram describing the electronic properties of |(OEP)Ce^{IV}-

(28) Shannon, R. D.; Prewitt, C. T. *Acta Crystallogr., Sect. B: Struct. Crystallogr. Cryst. Chem.* **1969**, *B25*, 928.

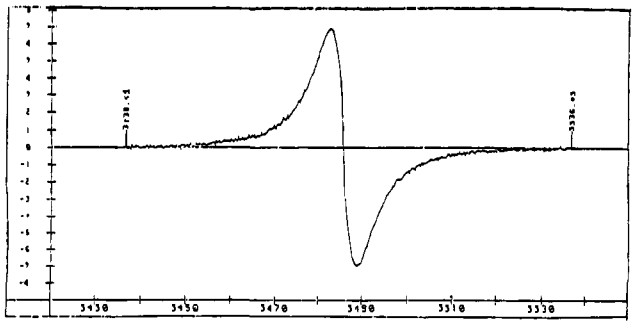

Figure 3. Electron spin resonance spectrum of |(TPP)La(Pc)| (**1**(La)) at 300 K in the solid state.

$(TPP)|^+$ can also be applied to the heteroleptic |(TPP)M(Pc)| species. In C_{4v} symmetry, if $\pi-\pi$ interactions are present, the near-IR band would be due to an intradimer electronic transition of the a_2 (bonding) $\rightarrow$ a_2^* (antibonding) type. Consequently, the electron hole would not reside exclusively on a phthalocyanine ring, but in a dimer molecular orbital whose composition is determined by the relative energies of the phthalocyanine and tetraphenylporphyrin monomer orbitals of appropriate symmetry and by the interaction between them. The resonance Raman properties of the heteroleptic |(TPP)Gd(Pc)| complex seem to indicate that only weak $\pi-\pi$ interactions are present in such complexes. Indeed, the intense 1500 cm^{-1} band present in the resonance Raman spectra of metallophthalocyanines $C_\beta-C_\beta$ and $C_\alpha-N_m$ character and is up-shifted by 18 cm^{-1} when going from |Mg(Pc)| to $|Mg(Pc)|^+$. Since, a similar shift (15 cm^{-1}) occurs between $|(TPP)Gd(Pc)|^-$ and |(TPP)Gd(Pc)|,[8] the contribution of the phthalocyanine a_{1u} highest occupied monomer molecular orbital to the dimer molecular orbital must be quite large and varies with the ionic radii of the tervalent metals. Consequently, we can assume that the electron hole present in the heteroleptic |(TPP)M(Pc)| sandwich complexes is mainly localized at the phthalocyanine ring.

The UV–vis spectrum obtained in dichloromethane (Figure 1b) of the light-green protonated form **1**[H](La) resembles that of the reduced light-green double-decker species $|(TPP)La(Pc)|^-$ **2**(La). This complex **2**(La) can be obtained by reduction of the neutral nonprotonated form **1**(La) with hydrazine (see Experimental Section). The reduction of **1**(La) seems again to take place mainly at the phthalocyanine ring, as indicated by the disappearance of the bands lying at 484, 965, and 1535 nm (near-IR) in the UV–vis and near-IR spectra of **1**(La).

The presence of an unpaired spin in these heteroleptic |(TPP)M(Pc)| complexes has been confirmed by EPR spectroscopy. The neutral, nonprotonated states **1** of all these complexes display in the solid state, at normal temperature, an EPR spectrum with a signal having a g of 2.0023 (Figure 3), typical for an organic radical.

In order to confirm that the electron hole is mainly localized at the phthalocyanine ring in these |(TPP)M(Pc)| complexes, we have studied their IR spectral properties. Figure 4a displays the IR spectrum of |(TPP)Lu(Pc)| (**1**(Lu)). It was shown, several years ago, that a TPP π-radical displays a band in the IR lying between 1270 and 1295 cm^{-1} whereas under similar conditions an OEP π-radical absorbs between 1520 and 1570 cm^{-1}.[31-33] A similar band located at 1310 cm^{-1} appears in the IR spectrum of the one-electron-oxidized actinide heteroleptic sandwich

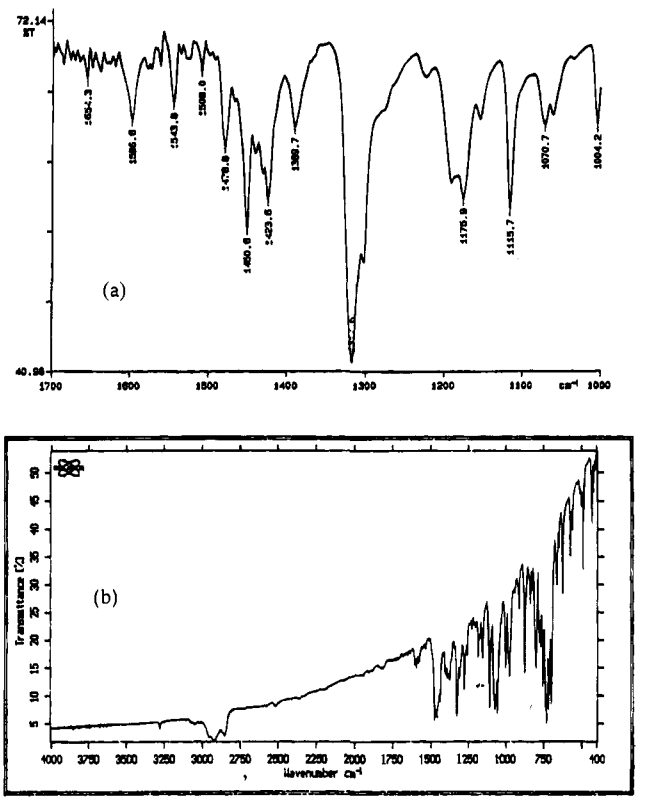

Figure 4. Solid state infrared spectra of (a) |(TPP)Lu(Pc)| (**1**(Lu)) and (b) |(TPP)LaH(Pc)| (**1**(H)(La)).

complex $|(TPP)U^{IV}(Pc)|^+$. It has been suggested by Kadish et al.[7] that this band indicates the presence of a phthalocyanine monoanion, $Pc^{\bullet-}$, as a ligand.

The neutral, nonprotonated states **1** of all the heteroleptic |(TPP)M(Pc)| complexes that we have studied, in which one of the tetrapyrrole ligands is oxidized into a π-radical, present a strong IR spectral band at 1317 cm^{-1}. In contrast, in the neutral states of the tetravalent-metal sandwich derivatives, such as $|(Pc)U^{IV}(Pc)|$ and $|(TPP)Ce^{IV}(Pc)|$, containing two nonoxidized tetrapyrrole ligands, such a band appears at 1328 cm^{-1}. Furthermore, the neutral, nonprotonated states **1** of the |(TPP)M(Pc)| complexes present no IR spectral band lying between 1270 and 1295 cm^{-1} attributable to the presence of a TPP π-radical. Consequently, the absence of an IR band lying in this range confirms that the π-radical must be mainly localized on the phthalocyanine ring, and the presence of an IR spectral band lying at 1317 cm^{-1} is also consistent with the localization of the unpaired spin, present in the neutral states **1** of the heteroleptic tervalent-metal derivatives |(TPP)M(Pc)|, on the phthalocyanine ligand.

The IR spectrum of the protonated form **1**[H](La) (Figure 4b) shows a band at 1328 cm^{-1}. The position of this band is consistent with the presence of a nonoxidized dianionic phthalocyanine ligand. Another band appears at 3280 cm^{-1}, which is absent in the spectra of the neutral, nonprotonated form **1** of the |(TPP)Ln(Pc)| complexes. It corresponds, most probably, to an N–H stretching vibration. Its presence indicates that one of the tetrapyrrole ligands has been protonated. A similar band is present at 3300 cm^{-1} in the IR spectra of |(TPP)LaH(TPP)| and |(OEP)LaH(OEP)|[34] and at 3290 cm^{-1} in the IR spectra of |(OEP)PrH(OEP)| and |(OEP)PrH(TPP)|.[34,35]

(29) (a) Konami, H.; Hatano, M.; Kobayashi, N.; Osa, T. *Chem. Phys. Lett.* **1990**, *165*, 397. (b) Donohoe, R. J.; Duchowski, J. K.; Bocian, D. F. *J. Am. Chem. Soc.* **1988**, *110*, 6119. (c) Martin, P. C.; Arnold, J.; Bocian, D. F. *J. Phys. Chem.* **1993**, *97*, 1332. (d) Bilsel, O.; Rodriguez, J.; Milam, S. N.; Gorlin, P. A.; Girolami, G. S.; Suslick, K. S.; Holten, D. *J. Am. Chem. Soc.* **1992**, *114*, 6528.

(30) Duchowski, J. K.; Bocian, D. F. *Inorg. Chem.* **1990**, *29*, 4158.

(31) Scholz, W. F.; Reed, C. A.; Lee, Y. J.; Scheidt, W. R.; Lang, G. *J. Am. Chem. Soc.* **1982**, *104*, 6791.

(32) Shimomura, E. T.; Phillippi, M. A.; Goff, H. M. *J. Am. Chem. Soc.* **1981**, *103*, 6778.

(33) Kadish, K. M.; Mu, X. H. *Pure Appl. Chem.* **1990**, *62*, 1051.

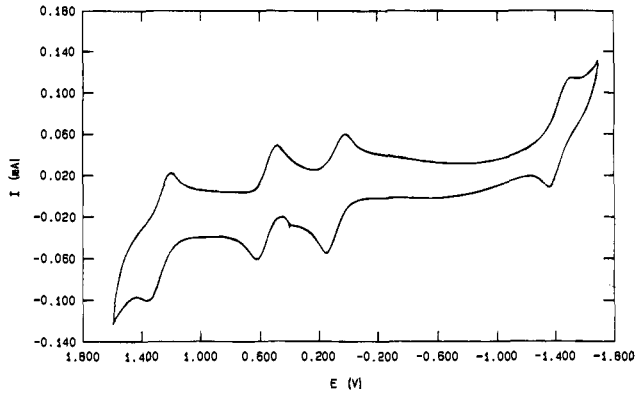

Figure 5. Cyclic voltammogram of |(TPP)Gd(Pc)| (**1**(Gd)) in CH_2Cl_2 (0.1 M NBu_4PF_6), voltage scan rate 0.1 V/s.

Table 3. Redox Potentials (V vs SCE) of the |(TPP)M(Pc)| (**1**) Complexes (M = La, Pr, Nd, Eu, Gd, Er, Lu, and Y) in Correlation with the Ionic Radii r_i (Å) of M^{III}

	r_i	E_{ox}^1	E_{ox}^2	E_{red}^1	E_{red}^2
M = La	1.18	0.67	1.275	0.195	−1.395
Pr	1.14	0.63	1.28	0.16	−1.41
Nd	1.12	0.615	1.28	0.14	−1.415
Eu	1.07	0.535	1.28	0.09	−1.435
Gd	1.06	0.555	1.28	0.085	−1.435
Y	1.015	0.51	1.28	0.04	−1.45
Er	1.00	0.495	1.275	0.025	−1.46
Lu	0.97	0.465	1.275	0.00	−1.465

Cyclic Voltammetry and Spectroscopic Properties of the One-Electron-Reduced and -Oxidized States. The redox behavior of the neutral, nonprotonated states **1** of the |(TPP)M(Pc)| complexes was determined by cyclic voltammetry in dichloromethane. A typical voltammogram (|(TPP)Gd(Pc)|) is given in Figure 5. Generally, four reversible one-electron processes are found for these complexes which are represented by the following five redox states:

$$|(TPP)M(Pc)|^{2-} \underset{}{\overset{E_{red}^2}{\rightleftharpoons}} |(TPP)M(Pc)|^{-} \overset{E_{red}^1}{\rightleftharpoons}$$
green light-green

$$|(TPP)M(Pc)| \overset{E_{ox}^1}{\rightleftharpoons} |(TPP)M(Pc)|^{+} \overset{E_{ox}^2}{\rightleftharpoons} |(TPP)M(Pc)|^{2+}$$
red-brown red blood-red

The individual half-wave potentials $E_{ox}^{1,2}$ and $E_{red}^{1,2}$ for the different redox processes are displayed in Table 3. The one-electron-oxidized and -reduced species were generated by chemical or electrochemical methods, isolated as $(SbCl_6)^-$ and $(NBu_4)^+$ salts, respectively (see Experimental Section), and identified spectroscopically and by single crystal X-ray diffraction for $|(TPP)Gd(Pc)|^+|SbCl_6|^-$. The half-wave potential E_{ox}^1 corresponding to a reversible one-electron oxidation of the neutral form **1** of |(TPP)M(Pc)| and the half-wave potentials E_{red}^1 and E_{red}^2 corresponding, respectively, to reversible one- and two-electron reductions of **1** may be correlated with the radii of the tervalent central metals. Indeed, as shown in Figure 6, the redox potentials E_{ox}^1, E_{red}^1, and E_{red}^2 decrease linearly with increasing radii of the central metals in the same manner as the energies of the near-IR bands (Figure 2a). Hence, they are also dependent on the ring to ring interseparations. The importance of the size of the central metal is exemplified by the observation that the data for |(TPP)Y(Pc)| fit the linear correlation observed for the lanthanide derivatives |(TPP)M-

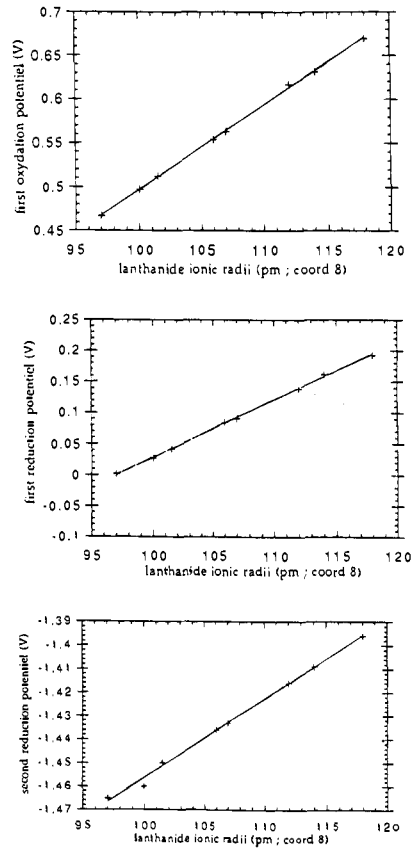

Figure 6. First oxidation potential E_{ox}^1 and first and second reduction potentials E_{red}^1 and E_{red}^2 of |(TPP)M(Pc)| (**1**) complexes (V; in 0.1 M NBu_4PF_6/CH_2Cl_2 vs SCE) as functions of the ionic radii r_i (pm; octacoordinated) of the tervalent central metal M.

(Pc)| (M = La, Pr, Nd, Eu, Gd, Er, Lu). The linear correlation observed between E_{ox}^1, E_{red}^1, and E_{red}^2 and the radii r_i of the central metals again indicates that $\pi-\pi$ interactions are probably present in these heteroleptic |(TPP)M(Pc)| sandwich derivatives (vide supra).

Table 2b gives the wavelengths of the UV−vis spectral band maxima found for the singly reduced states $|(TPP)M(Pc)|^-$ **2**. A typical UV−vis spectrum ($|(TPP)Pr(Pc)|^-$) is represented in Figure 1c. The four bands located at 574, 598, 636, and 770 nm are attributed to the Q bands of the phthalocyanine ring. The bands lying at 550 and 650 nm contain, most probably, a contribution from the Q bands of the porphyrin macrocycle. The Soret bands of the porphyrin (416 nm) and phthalocyanine (336 nm) ligands are red-shifted relative to those appearing in the spectrum of the neutral form of |(TPP)Pr(Pc)| at 410 and 325 nm. The origins of the bands lying at 379 and 479 nm are not clear. A band located close to 379 nm is also present in the corresponding lanthanide bisphthalocyanine derivatives $|(Pc)Ln^{III}(Pc)|^-$,[1a,b,36] and the band at 479 nm could correspond to a $\pi \rightarrow \pi^*$ transition between the two interacting tetrapyrrole macrocycles.[8,37] The IR spectra of **2** show a band at 1328 cm^{-1}. The presence of this band is a confirmation that the phthalocyanine ligand is dianionic in the singly reduced states **2**. The one-electron reduction potentials E_{red}^1 of species **1**, which range from 0.002 to 0.193 V (SCE) (Table 3) for the different metals, are quite small. A small amount of hydrazine in DMF (DMF + 1% N_2H_4) in the presence of NBu_4PF_6 allows the reduction of the red-brown |(TPP)M(Pc)| (**1**) derivatives into the light-

(34) Buchler, J. W.; Kihn-Botulinski, M.; Löffler, J.; Scharbert, B. *New J. Chem.* **1992**, *16*, 545.
(35) Buchler, J. W.; Kihn-Botulinski, M.; Scharbert, B. *Z. Naturforsch.* **1988**, *43B*, 1371.
(36) Konami, H.; Hatano, M.; Tajiri, A. *Chem. Phys. Lett.* **1989**, *160*, 163.
(37) Bilsel, O.; Buchler, J. W.; Hammerschmitt, W. P.; Rodriguez, J.; Holten, D. *Chem. Phys. Lett.* **1991**, *182*, 415.

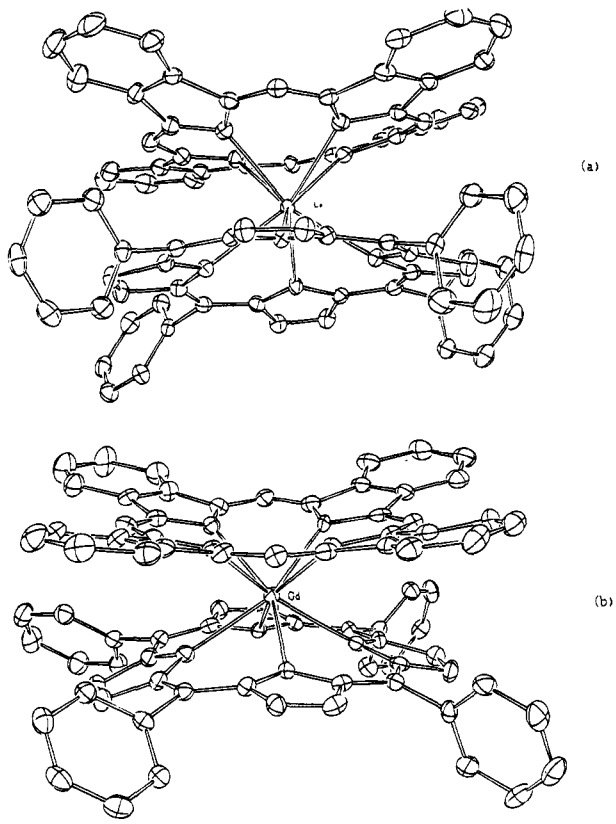

Figure 7. ORTEP plots of (a) |(TPP)La(Pc)| and (b) |(TPP)Gd(Pc)|$^+$. Ellipsoids are scaled to enclose 30% of the electronic density. Hydrogen atoms are omitted.

green |(TPP)M(Pc)|$^-$ **2** species. The lanthanum derivative |(TPP)La(Pc)|$^-$ **2**(La) can also be obtained by deprotonation of the protonated form **1**[H](La) with sodium ethoxide.

The red singly oxidized species **3** were prepared by electrolysis of a dichloromethane solution of the neutral, nonprotonated complexes **1** at a constant potential of +0.7 V (SCE) or by chemical oxidation of the neutral species **1** with a dichloromethane solution of phenoxathiinylium hexachloroantimonate. The wavelengths of the band maximas appearing in the UV–vis spectra of these red derivatives |(TPP)M(Pc)|$^+$ **3** are given in Table 2c. Figure 1d shows a typical spectrum of such a one-electron-oxidized complex |(TPP)Er(Pc)|$^+$|$SbCl_6$|$^-$). These derivatives **3** are di-π-radicals. The IR spectra of these singly oxidized species |(TPP)M(Pc)|$^+$ **3** display, in addition to the band at 1317 cm^{-1} which was attributed to the presence of a phthalocyanine π-radical, Pc$^{\bullet-}$ (vide supra), a band at 1258 cm^{-1} which indicates the presence of a tetraphenylporphyrin π-radical, TPP$^{\bullet-}$. As indicated before (vide supra), TPP$^{\bullet-}$ π-radicals display a band in the IR lying between 1270 and 1295 cm^{-1} whereas under similar conditions an OEP$^{\bullet-}$ π-radical shows an IR absorption band between 1520 and 1570 cm^{-1}.[31-33] Furthermore, these derivatives |(TPP)M(Pc)|$^+$ **3** are still highly paramagnetic, a property which excludes the presence of a phthalocyanine di-π-cation. Thus, the singly-oxidized forms **3** of these heteroleptic tervalent-metal porphrin–phthalocyanine complexes **1** are porphyrin and phthalocyanine π-cation radical species. As shown in Figure 2b, a linear correlation is also observed between the ionic radii of the central metals and the wavenumbers of the near-IR bands for these one-electron-oxidized species **3** (Table 2b). The paramagnetic properties of these |(TPP)M(Pc)|$^+$ complexes can be explained by the orthogonalities of the Pc$^{\bullet-}$ and TPP$^{\bullet-}$ magnetic orbitals. These

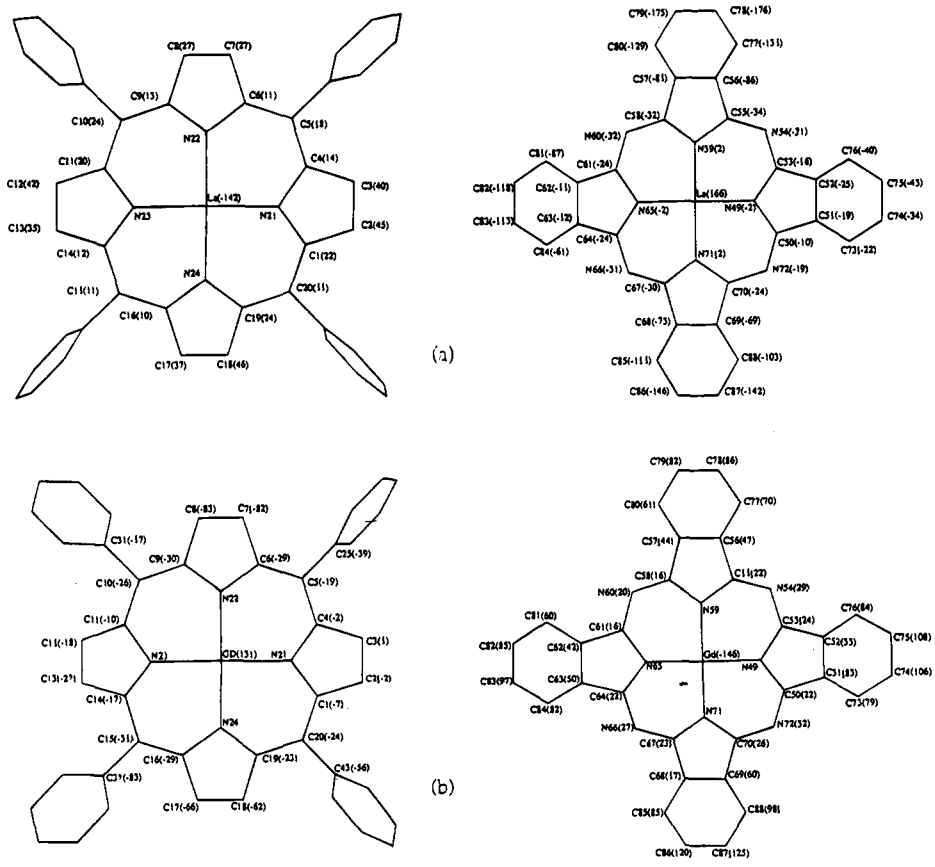

Figure 8. Stick bond model projection of TPP and Pc rings in (a) |(TPP)La(Pc)| (**1**(La)) and (b) |(TPP)Gd(Pc)|$^+$ **3**(Gd) giving the labeling schemes of all the atoms, except hydrogens. The displacements are indicated relative to the $4N_p$ and $4N_{iso}$ mean planes of the porphyrin and phthalocyanine rings.

Table 4. Selected Bond Distances and Angles in |(TPP)La(Pc)|

	Bond Lengths (Å)		
La−N(21)	2.528(3)	La−N(49)	2.594(3)
La−N(22)	2.526(3)	La−N(59)	2.603(3)
La−N(23)	2.524(3)	La−N(65)	2.594(3)
La−N(24)	2.505(3)	La−N(71)	2.569(3)
	Bond Angles (deg)		
N(21)−La−N(22)	70.70(9)	N(49)−La−N(59)	65.25(9)
N(21)−La−N(23)	111.12(9)	N(49)−La−N(65)	99.62(9)
N(21)−La−N(24)	71.94(9)	N(49)−La−N(71)	66.13(9)
N(22)−La−N(23)	71.27(9)	N(59)−La−N(65)	66.02(9)
N(22)−La−N(24)	111.15(9)	N(59)−La−N(71)	101.38(9)
N(23)−La−N(24)	71.52(9)	N(65)−La−N(71)	66.09(9)
N(21)−La−N(49)	141.56(9)	N(21)−La−N(59)	143.97(9)
N(21)−La−N(65)	82.79(9)	N(21)−La−N(71)	80.54(9)
N(22)−La−N(49)	86.69(9)	N(22)−La−N(59)	145.25(9)
N(22)−La−N(65)	142.97(9)	N(22)−La−N(71)	83.99(9)
N(23)−La−N(49)	89.08(9)	N(23)−La−N(59)	87.45(9)
N(23)−La−N(65)	144.56(9)	N(23)−La−N(71)	146.09(9)
N(24)−La−N(49)	146.48(9)	N(24)−La−N(59)	86.27(9)
N(24)−La−N(65)	83.19(9)	N(24)−La−N(71)	141.00(9)

Table 5. Selected Bond Distances and Angles in $|(TPP)Gd(Pc)|^+$

	Bond Lengths (Å)		
Gd−N(21)	2.447(7)	Gd−N(49)	2.446(7)
Gd−N(22)	2.464(7)	Gd−N(59)	2.450(7)
Gd−N(23)	2.448(7)	Gd−N65)	2.457(7)
Gd−N(24)	2.451(7)	Gd−N(71)	2.449(7)
	Bond Angles (deg)		
N(21)−Gd−N(22)	73.0(2)	N(49)−Gd−N(59)	69.4(2)
N(21)−Gd−N(23)	114.9(2)	N(49)−Gd−N(65)	106.8(2)
N(21)−Gd−N(24)	73.3(2)	N(49)−Gd−N(71)	69.5(2)
N(22)−Gd−N(23)	73.6(2)	N(59)−Gd−N(65)	68.6(2)
N(22)−Gd−N(24)	116.1(2)	N(59)−Gd−N(71)	106.9(2)
N(23)−Gd−N(24)	74.0(2)	N(65)−Gd−N(71)	69.2(2)
N(21)−Gd−N(49)	78.0(2)	N(21)−Gd−N(59)	137.4(2)
N(21)−Gd−N(65)	149.9(2)	N(21)−Gd−N(71)	85.7(2)
N(22)−Gd−N(49)	84.7(2)	N(22)−Gd−N(59)	77.2(2)
N(22)−Gd−N(65)	136.4(2)	N(22)−Gd−N(71)	149.6(2)
N(23)−Gd−N(49)	149.0(2)	N(23)−Gd−N(59)	84.1(2)
N(23)−Gd−N(65)	76.6(2)	N(23)−Gd−N(71)	136.3(2)
N(24)−Gd−N(49)	136.6(2)	N(24)−Gd−N(59)	148.7(2)
N(24)−Gd−N(65)	84.5(2)	N(24)−Gd−N(71)	76.4(2)

orbitals have, respectively, a_2 and a_1 symmetry in the C_{4v} point group of the $|(TPP)M(Pc)|^+$ molecules. The magnetic properties and ferromagnetic spin−spin exchange interactions (if present), which have not been studied as yet, could help to evaluate the strength of the $\pi-\pi$ interactions occurring between the tetrapyrrole ligands in these heteroleptic |(TPP)M(Pc)| and $|(TPP)M(Pc)|^+$ complexes.

Crystal and Molecular Structures of 1(La)·2CH_2Cl_2 and 3(Gd)($SbCl_6$)·2(CH_2Cl_2), (H_2O). ORTEP plots of the molecular structures of 1(La)·2CH_2Cl_2 and 3(Gd)($SbCl_6$)·2(CH_2Cl_2),-(H_2O) are displayed in Figure 7. Figure 8 gives for each derivative the labeling schemes used for the atoms, except the hydrogens, and indicates the displacements in 0.01 Å of the porphyrin core atoms relative to their four pyrrole nitrogen mean planes and of the phthalocyanine core atoms relative to their four isoindole nitrogen mean planes. Selected bond distances and bond angles are given for each complex in Tables 4 and 5, respectively.

Each metal cation is octacoordinated, bonded to four pyrrole nitrogens of one porphyrin ring and to four isoindole nitrogens of one phthalocyanine ring. Both tetrapyrrole rings of each derivative adopt a staggered orientation with relative rotation angles of 45.7(2)° in 1(La)·2CH_2Cl_2 and 37.1(3)° in 3(Gd)($SbCl_6$)·2(CH_2Cl_2),(H_2O). Consequently, the coordination environment of each metal cation is a slightly distorted square antiprism. The average metal−nitrogen distances are, for 1(La)·2CH_2Cl_2, La−N_p = 2.520(3) Å and La−N_{iso} = 2.590(3) Å and, for 3(Gd)($SbCl_6$)·2(CH_2Cl_2),(H_2O), Gd−N_p = 2.452(7) Å and Gd−N_{iso} = 2.450(7) Å. In 1(La)·2CH_2Cl_2, the metal cation lies 1.425(2) Å above the four pyrrole nitrogen mean planes $4N_p$ and 1.656(2) Å below the four isoindole nitrogen mean planes $4N_{iso}$. In 3(Gd)($SbCl_6$)·2(CH_2Cl_2),(H_2O) these distances are 1.309(5) and 1.460(5) Å, respectively. A close examination of the $Ln^{III}-N_{iso}$ mean bond distances in the known X-ray structures of the octacoordinated lanthanide metal bisphthalocyanine sandwich derivatives containing two dianionic Pc^{2-} ligands [$|Ce^{III}(Pc)_2|^-$ (2.54 Å),[38] $|Lu(Pc)_2|^-$ (2.38 Å),[39] |Lu(H)$(Pc)_2$| (2.37 Å)[39]] shows, by substraction of the metal radii,[28] that the radius of N_{iso} lies between 1.40 and 1.41 Å and is not significantly different in the heteroleptic neutral |(TPP)-La(Pc)| (1.41 Å) and oxidized $|(TPP)Gd(Pc)|^+$ (1.39 Å) complexes. Hence, the mean Ln−N_{iso} bond distances cannot be used to find out on which tetrapyrrole ligand the π-radical resides.

In each derivative, the porphyrin rings are domed. The $4N_p$ mean planes of these rings are displaced by 0.314(2) (1(La)·2CH_2-Cl_2) and 0.245(5) (3(Gd)($SbCl_6$)·2(CH_2Cl_2),(H_2O)) Å with respect to the 24-atom-core mean planes of each ring. The dihedral angles of the pyrrole rings range from 7.40(3)° to 10.77-(3)° (mean value 9.87(3)°) in 1(La)·2CH_2Cl_2 and from 2.18-(3)° to 21.80(3)° (mean value 11.46(3)°) in 3(Gd)($SbCl_6$)·2(CH_2-Cl_2),(H_2O). Thus, the porphyrin ring of 3(Gd)(Sb-Cl_6)·2(CH_2Cl_2),(H_2O) is severely distorted relative to that present in 1(La)·2CH_2Cl_2. However, the distortion of this ring is not, necessarily, related the porphyrin π-radical nature of this ligand in this complex.

The phthalocyanine macrocycles are also domed in both complexes and display a saucer shape. Despite the probable localization of the π-radical on the phthalocyanine rings in 1(La)·2CH_2Cl_2 and 3(Gd)($SbCl_6$)·2(CH_2Cl_2),(H_2O), the structures of this ring are not significantly different from those found in several divalent metallophthalocyanines in which these rings are dianionic ligands.[40]

Supporting Information Available: Tables S1 (positional parameters and their ESDs), S2 (thermal parameters for anisotropic atoms), S3 (hydrogen atom positional parameters), S4 (complete set of bond distances (Å)), and S5 (complete set of bond angles (deg)) for 1(La)·2CH_2Cl_2 and Tables S7 (positional parameters and their ESDs), S8 (thermal parameters for anisotropic atoms), S9 (hydrogen atom positional parameters), S10 (complete set of bond distances (Å)), and S11 (complete set of bond angles (deg)) for 3(Gd)($SbCl_6$)·2(CH_2Cl_2),(H_2O) (37 pages); observed and calculated structure factor amplitudes for all observed reflections (×10) (Tables S6 and S12 for 1(La)·2CH_2-Cl_2 and 3(Gd)($SbCl_6$)·2(CH_2Cl_2),(H_2O), respectively) (53 pages). This material is contained in many libraries on microfiche, immediately follows this article in the microfilm version of the journal, can be ordered from the ACS, and can be downloaded from the Internet; see any current masthead page for ordering information and Internet access instructions.

JA9440361

(38) Lachkar, M. Thesis, Université Louis Pasteur, Strasbourg, 1988.
(39) Moussavi, M.; De Cian, A.; Fischer, J.; Weiss, R. *Inorg. Chem.* **1988**, *27*, 1287.
(40) Hoskins, B. F.; Mason, S. A.; White, J. B. C. *J. Chem. Soc., Chem. Commun.* **1969**, 554.